Eur Respir J 2006; 27: 268–275
DOI: 10.1183/09031936.06.00072005

Assessment of right ventricular function by strain rate imaging in chronic obstructive pulmonary disease

A. Vitarelli, Y. Conde, E. Cimino, S. Stellato, S. D'Orazio, I. D'Angeli, B.L. Nguyen, V. Padella, F. Caranci, A. Petroianni, L. D'Antoni and C. Terzano

ABSTRACT: The purpose of the current study was to compare right ventricular (RV) myocardial wall velocities (tissue Doppler imaging) and strain rate imaging (SRI) parameters with conventional echocardiographic indices evaluating RV function in chronic obstructive pulmonary disease (COPD) patients.

In total, 39 patients with COPD and 22 healthy subjects were included in the current study. Seventeen patients had pulmonary artery pressure <35 mmHg (group I) and 22 patients had pulmonary artery pressure >35 mmHg (group II). Tissue Doppler imaging, strain and strain rate (SR) values were obtained from RV free wall (FW) and interventricular septum. Respiratory function tests were performed (forced expiratory volume in one second/vital capacity (FEV_1/VC) and carbon monoxide diffusion lung capacity per unit of alveolar volume ($D_{L,CO}/V_A$)).

Strain/SR values were reduced in all segments of group II patients compared with group I patients and controls with lowest values at basal FW site. A significant relationship was shown between peak systolic SR at basal FW site and radionuclide RV ejection fraction. A significant relationship was shown between peak systolic SR at basal FW site and $D_{L,CO}/V_A$ and FEV_1/VC.

In conclusion, in chronic obstructive pulmonary disease patients, strain rate imaging parameters can determine right ventricular dysfunction that is complementary to conventional echocardiographic indices and is correlated with pulmonary hypertension and respiratory function tests.

KEYWORDS: Echocardiography, cor pulmonale, pulmonary function tests, right ventricular function, strain Doppler imaging

The evaluation of right ventricular (RV) function is clinically useful in patients with chronic obstructive pulmonary disease (COPD) because the presence of RV failure has prognostic implications [1, 2]. All invasive and noninvasive techniques evaluating RV performance have important limitations due to the complex geometry of the right ventricle [3–15]. The introduction of Doppler measurement of myocardial wall velocities (tissue Doppler imaging; TDI) and the recently developed strain rate imaging (SRI) technique have made a more adequate assessment of global and regional systolic and diastolic RV function possible [16–23]. The purpose of the present study was: 1) to compare SRI parameters with conventional echocardiographic indices and radionuclide indices evaluating RV function in COPD patients; and 2) to assess the correlation among SRI parameters and respiratory function tests.

METHODS

Population

In total, 39 patients (aged 54±13 yrs) with COPD were included in the study. On the basis of Doppler peak regurgitation velocity [24], patients were divided into two groups. Seventeen patients had pulmonary artery pressure <35 mmHg (group I) and 22 patients had pulmonary artery pressure >35 mmHg (group II). Cor pulmonale was defined in clinical terms as the presence of peripheral oedema in association with chronic obstructive lung disease for which no other cause could be found. None of the patients studied had clinical evidence of cor pulmonale and none of them was studied during an exacerbation of their chronic obstructive lung disease. None of the patients had clinical or electrocardiographic evidence of systemic hypertension, myocardial ischaemia or valvular heart disease. Cardiac drugs were withdrawn 24 h

AFFILIATIONS
''La Sapienza'' University, Rome, Italy.

CORRESPONDENCE
A. Vitarelli
Via Lima 35
00198 Rome
Italy
Fax: 39 068841926
E-mail: vitar@tiscali.it

Received:
June 18 2005
Accepted after revision:
September 22 2005

SUPPORT STATEMENT
This study was presented in part at the Heart Failure Society of America meeting, Toronto, Canada, September 12–15, 2004.

European Respiratory Journal
Print ISSN 0903-1936
Online ISSN 1399-3003

before the echocardiographic examination, whereas respiratory drugs, such as β_2-agonists, theophylline, inhaled steroids and oxygen therapy, were not discontinued. Twenty-two age- and sex-matched healthy subjects who had normal cardiac findings served as controls.

Echocardiography

All patients underwent a complete clinical examination as well as transthoracic echocardiography (Aplio echocardiograph; Toshiba Co., Tokyo, Japan). Measurements of right heart chambers were made by transthoracic echocardiography according to established criteria [7, 25]. RV end-diastolic (ED) area and end-systolic (ES) area were assessed by manual planimetry and RV fractional area change (RVFA) was derived using the following formula:

$$RVFA = (RVED_{area} - RVES_{area})/RVED_{area} \times 100 \quad (1)$$

RV volumes were calculated [5] with the difference-of-ellipsoids formula ($2/3 \times area \times length$) from the apical four-chamber (4-CH) view and either a parasternal short-axis or a subcostal-sagittal view and right ventricular ejection fraction (RVEF) was derived. Tricuspid annular plane systolic excursion was measured in the apical 4-CH view. Care was taken to avoid echo drop-outs of endocardial edges in regions of the tricuspid annulus and RV apex. The distance between the tricuspid annulus and the RV apex was measured at end-diastole and end-systole of the same cardiac cycle, and tricuspid annular plane systolic excursion was calculated as the difference between ED and end-systolic measurements [26].

Trans-tricuspid valve Doppler flow velocities were recorded at a speed of 100 $mm \cdot s^{-1}$ from the apical 4-CH view using the same machine and transducer in the pulsed-wave Doppler mode, with the sample volume positioned at the tips of the trans-tricuspid valve leaflets. Peak early and late diastolic velocities were measured. The average of six cycles was used to minimise differences during the breath cycle. RV isovolumic relaxation time was determined as the period from pulmonary valve closure to tricuspid valve opening. Deceleration time was calculated as the time interval from the peak E to the extrapolation of the early deceleration phase to the baseline [27]. In patients with summation of E and A waves, deceleration time of early diastolic filling was not recorded. Pulmonary artery systolic pressure was estimated by continuous wave Doppler as peak regurgitation velocity plus assumed right atrial pressure of 10 mmHg (fixed-value method) [24]. For the analysis of global RV function, Doppler parameters were used to derive the Tei index as previously described [28, 29]. Tricuspid closure time was measured as the time interval between the tricuspid valve closure and opening clicks.

Tissue Doppler imaging

The general principles that underlie the TDI modalities have been previously described [30]. Briefly, by excluding the low-intensity flow signals, the strong tissue signals derived from ventricular wall motion are sent directly into the autocorrelator without high-pass filtering. Recordings were stored digitally as two-dimensional (2D) cineloops and transferred to an optical disk medium for off-line analysis. The images showing the tissue motion velocity were superimposed on the 2D echocardiographic image for real-time colour display.

By using the transthoracic apical 4-CH views, the ventricular wall motion velocities were assessed during the cardiac cycle. Velocities toward the transducer are colour-coded red, and velocities away from the transducer are colour-coded blue. 2D tissue velocity images of the ventricular wall were obtained at 120 ± 15 $frames \cdot s^{-1}$, which implies a temporal resolution of ~15 ms. By marking a region of interest on the 2D image, velocities throughout the cardiac cycle for this area can be determined. The raw data were digitally stored and offline analysis of the data sets was performed using dedicated software.

TDI wall velocities during systole, early relaxation (E_W) and atrial systole (A_W) were processed from RV free wall (FW) and interventricular septum at three sites (basal, mid cavity and apical) in the apical 4-CH view (fig. 1a).

The strain (change in length per unit length) in each segment was defined [23] as the relative magnitude of segmental deformation. From tissue Doppler data, strain rate (SR; velocity of segmental deformation) can be estimated by calculating the velocity gradient. The time integral of incremental SR yields logarithmic strain:

$$e = \log(L/L_0) \quad (2)$$

FIGURE 1. Two-dimensional tissue Doppler image with sample site in the right ventricular free wall (apical four-chamber view). a) Velocities profiles: the systolic (S), early diastolic (E) and atrial (A) induced velocities are shown. b) Strain rate profiles: S, E and A induced strain rate values are shown. c) Strain profiles indicating systolic strain (SS) are shown.

In the present study, the logarithmic strain was converted to Lagrangian strain:

$$\varepsilon = (L - L_0)/L_0 \quad (3)$$

The velocity gradient was estimated between two points with a distance of 12 mm. This spatial offset was selected as a compromise between acceptable signal-to-noise ratio and longitudinal spatial resolution.

SR was determined during isovolumic contraction, systole (S), isovolumic relaxation, early diastole (E) and late diastole (A; fig. 1b). SS was measured from the same wall site in the same views (fig. 1c). TDI wall velocities at the tricuspid annulus level during systole, early relaxation and atrial systole were also obtained. To minimise the effect of respiration on variability, all calculations were performed using the mean of six or seven clearly observed consecutive beats.

Pulmonary function tests

Echocardiographic parameters were evaluated after the respiratory function tests were performed (forced expiratory volume in one second/vital capacity (FEV_1/VC); carbon monoxide diffusion capacity per unit of alveolar volume ($D_{L,CO}/V_A$)).

Radionuclide angiography

Echocardiographic parameters of RV longitudinal function were compared in 23 patients using estimates of the RVEF obtained by radionuclide imaging. A semi-automatic commercially available program (GE protocol; GE Medical Systems, Milwauke, WI, USA) was used for nuclear analysis. Maximum and minimum values of the background corrected time-activity curves were used for the calculations of the ejection fraction. The evaluation was performed by an experienced nuclear cardiologist blinded to the echocardiographic results.

Statistics

Data are presented as mean±SD. Linear correlations, univariate and multivariate analysis were used for comparisons. Comparisons between different regions were analysed using an unpaired t-test and differences were considered statistically significant when the p-value was <0.05. The cut-off values of strain and SR, enabling the prediction of RV systolic dysfunction (ejection fraction <50%) with the highest sensitivity and specificity, were identified by means of receiver operating characteristic curves of echocardiographic indexes [31]. To test intraobserver variability, measurements of systolic and diastolic TDI were made at 50 sites on two different occasions. For interobserver variability, a second investigator randomly made measurements at the above different sites without knowledge of other echocardiographic parameters. The intra- and interobserver variabilities were determined as the difference between the two sets of observations divided by the mean of the observations and expressed as a percentage.

RESULTS

Measurements of TDI/SRI parameters could be obtained in 39 out of 42 initially examined patients with a feasibility of 93%. The intraobserver error was low for wall velocities (4.3±3.7, 5.4±4.8 and 5.8±4.9% for peak systolic, peak early diastolic and peak late diastolic velocities, respectively), wall peak SS (4.9±3.8%) and SR (7.4±5.3, 4.4±3.5, 7.7±5.2, 5.7±4.3 and 6.2±5.1% for isovolumic contraction, systolic, isovolumic relaxation, early diastolic and late diastolic values, respectively). The interobserver error was also low for wall velocities (4.8±4.2, 6.2±5.3 and 6.8±5.5%, respectively), wall peak SS (5.2±3.9%) and SR values (7.9±5.4, 4.6±3.3, 8.1±5.2, 6.4±5.1 and 6.1%±5.6%, respectively). The reproducibility was relatively high for systolic velocity, SR and strain measurements, and lower for the diastolic measurements.

The patients' demographic data are given in table 1. The main echocardiographic features in the control and COPD groups are compared in tables 2 and 3.

Two-dimensional Doppler data

RVFA, RVEF, E/A ratio, deceleration time and tricuspid annular plane systolic excursion were not significantly different among the three groups (table 2). Isovolumic relaxation time and Tei index were lower in group II patients compared with controls ($p<0.05$). In group II patients, the mean RVEF was 51±4% (range, 28–63) and the mean RVFA was 39±7% (range, 23–43). Of the RV diastolic variables, isovolumic relaxation time was 119±12 ms (range, 47–157), deceleration time was 191±42 ms (range, 73–268) and Tei index was 0.58±0.13 (range, 0.36–0.92).

Tissue Doppler imaging/strain rate imaging data

Strain/SR values were reduced in all segments of group II patients compared with group I patients and controls with lowest values at basal free wall (FW) site (fig. 2). FW values were lower compared with interventricular septum values ($p<0.005$). E_W/A_W ratio at basal FW site was lower in group II patients (table 3) compared with controls ($p<0.01$). SS and peak systolic and diastolic SR at basal FW site (fig. 3, table 3) were significantly lower in group II patients than controls ($p<0.001$). TDI/SRI values were not obtained in one patient

TABLE 1 Patient characteristics

Characteristics	Values
Subjects	39
Age yrs	54±13
Sex	
Male	27 (69.2)
Female	12 (30.8)
Systolic BP mmHg	124.2±17.4
Diastolic BP mmHg	81.1±7.2
Abnormal ECG#	14 (36)
FEV_1/VC	58.9±19.3
$D_{L,CO}/V_A$	3.5±0.9
P_{a,CO_2} mmHg	39.9±5.8 (21.2–67.3)
P_{a,O_2} mmHg	61.8±7.9 (37.8–86.2)

Data are presented as mean±SD (range) or n (%). BP: blood pressure; ECG: electrocardiogram; FEV_1: forced expiratory volume in one second; VC: vital capacity; $D_{L,CO}$: single-breath diffusion capacity of the lung for carbon monoxide; V_A: alveolar volume; P_{a,CO_2}: arterial carbon dioxide tension; P_{a,O_2}: arterial oxygen tension;. #: ECG was considered abnormal if right-axis deviation, right bundle branch block, right ventricular hypertrophy, or P-pulmonale was present.

TABLE 2 Right ventricular two-dimensional Doppler echocardiographic parameters

	Controls	Patients with no PHT	Patients with PHT
Subjects n	22	17	22
Heart rate beats·min^{-1}	73±5	74±8	75±2
BSA m^2	1.71±0.27	1.75±0.11	1.72±0.89
RV and RA geometry			
RV free wall thickness mm	3±0.7	4±0.9	7±0.8**
RVEDD (M-mode) mm	10±0.3	12±0.14	29±0.11*
RVEDsax (2D-4-CH) mm	31±3	33±9	52±7**
RVEDlax (2D-4-CH) mm	66±5	74±3	94±9**
RAESsax (2D-4-CH) mm	38±4	41±2	47±6*
RAESlax (2D-4-CH) mm	42±4	44±5	53±5*
RV systolic function			
RV ejection fraction %	65±9	58±8	51±4
RV fractional area change %	45±6	43±8	39±7
TAPSE mm	21±3	19±6	16±4
RV diastolic function			
Peak E velocity cm·s^{-1}	81±8.3	78±12	77±19
Peak A velocity cm·s^{-1}	53±12	64±15	66±11
E/A ratio	1.5±0.4	1.2±0.9	1.1±0.6
IVRT ms	67±9	86±11	119±12*
DT ms	149±27	173±38	191±42
RV global function			
Tei index	0.29±0.03	0.37±0.11	0.58±0.13*

Data are presented as mean±SD. PHT: pulmonary hypertension; BSA: body surface area; RV: right ventricle; RA: right atrium; RVEDD: right ventricular end-diastolic diameter; RVEDsax: right ventricular end-diastolic short axis; 2D-4-CH: two-dimensional apical four-chamber view; RVEDlax: right ventricular end-diastolic long axis; RAESsax: right atrial end-systolic short axis; RAESlax: right atrial end-systolic long axis; TAPSE: tricuspid annulus plane systolic excursion; IVRT: isovolumic relaxation time; DT: deceleration time. *: p<0.05 *versus* controls; **: p<0.01 *versus* controls.

TABLE 3 Right ventricular tissue Doppler imaging/ strain rate (SR) imaging echocardiographic parameters

	Controls	Patients with no PHT	Patients with PHT
Subjects n	22	17	22
Heart rate beats·min^{-1}	73±5	74±8	75±2
BSA m^2	1.71±0.27	1.75±0.11	1.72±0.89
Sw velocity cm·s^{-1}#	9.5±1.6	7.9±1.7	5.8±1.9**
Ew velocity cm·s^{-1}#	-15.5±1.3	-12.9±2.4	-10.8±2.9*
Aw velocity cm·s^{-1}#	-2.7±1.4	-2.4±1.3	-2.2±1.5
Sa velocity cm·s^{-1}	8.4±1.7	6.9±1.2	6.1±1.4
Ea velocity cm·s^{-1}	-10.4±1.7	-8.4±1.2	-7.4±1.7
Aa velocity cm·s^{-1}	-2.4±1.7	-2.2±1.3	-2.1±1.8
Peak systolic wall strain %#	32.5±10.2	23.2±6.7*	19.5±7.9***
IVC wall SR s^{-1}#	2.9±1.8	2.4±1.6	1.9±1.7¶
Systolic wall SR s^{-1}#	-4.9±1.8	-3.3±1.6*	-2.9±1.5***
IVR wall SR s^{-1}#	2.4±1.7	1.9±1.2	1.6±1.4***
Early diastolic wall SR s^{-1}#	8.4±1.8	5.7±1.5*	4.4±1.7¶
Late diastolic wall SR s^{-1}#	2.7±1.7	2.1±1.8	2.1±1.6

Data are presented as mean±SD. PHT: pulmonary hypertension; BSA: body surface area; Sw: systolic wall; Ew: early diastolic wall; Aw: atrial wall; Sa: systolic annulus; Ea: early diastolic annulus; Aa: atrial annulus; IVC: isovolumic contraction; IVR: isovolumic relaxation. #: basal right ventrical free wall site; ¶: p<0.005 *versus* controls. *: p<0.05 *versus* controls; **: p<0.01 *versus* controls; ***: p<0.001 *versus* controls.

because of bad quality of the video recording. The Ew/Aw ratio, and Ew and Aw velocities were not evaluated in two patients due to high heart rates and merging early and late diastolic tricuspid velocity peaks.

Correlation with pulmonary function tests

Patients had a wide range of FEV1 and arterial blood gas tensions (table 1). The most significant relationship was shown (fig. 4) between peak systolic SR at basal FW site and $D_{L,CO}/V_A$ (r=0.75; p<0.001) and peak systolic SR at basal FW site and FEV1/VC (r=0.71; p<0.005). A significant correlation was also obtained between peak systolic SR at basal FW site and pulmonary artery systolic pressure (r=0.69; p<0.005). A cut-off point of mean SS and peak systolic SR at basal FW site of 25% and -4 s^{-1} had a sensitivity of 79 and 82%, and a specificity of 80 and 86%, respectively, in predicting normal systolic pulmonary artery pressure (⩽35 mmHg). There was a weak correlation between echocardiographic RVEF and carbon dioxide arterial tension (r=-0.27; p<0.01). There were no significant correlations between RVEF and arterial oxygen tension, FEV1, or $D_{L,CO}$ in the whole group of 39 patients or in any of the subgroups. No correlation was found between RVFA, E/A ratio, isovolumic relaxation time, deceleration time and respiratory function tests.

Correlation with radionuclide ventriculography

In the 23 patients that underwent radioisotopic examination, a significant relationship was shown between echocardiographic RVEF and radionuclide RVEF (r=0.63, p<0.005). A significant relationship was also shown between SS at basal FW site and radionuclide RVEF (r=0.78; p<0.001) and peak systolic SR at basal FW site and radionuclide RVEF (r=0.81; p<0.001). A cut-off point of mean SS and peak systolic SR at basal FW site of 25% and -4 s^{-1} had a sensitivity of 81 and 85%, and a specificity of 82 and 88%, respectively, in predicting preserved global ventricular systolic function (⩾0.50).

DISCUSSION

The current study shows that, in COPD patients, SRI parameters can determine RV dysfunction that is complementary to conventional echocardiographic indices and is correlated with severity of pulmonary disease.

Assessment of right ventricular function

RV hypertrophy and dilatation that occurs in COPD patients is a beneficial adaptation allowing the ventricle to cope with an increased afterload and maintain a normal cardiac output. Progressive RV dysfunction is associated with limited peripheral oxygen delivery and exercise capacity, and has an important bearing on prognosis that is independent of other

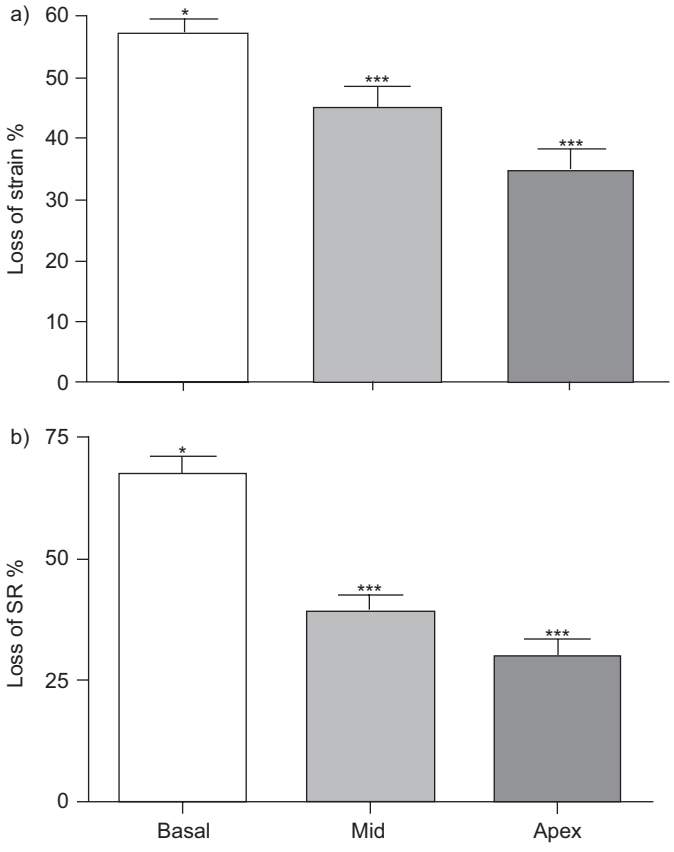

FIGURE 2. Loss of peak systolic strain (a) and strain rate (b), calculated as a percentage of normal control, at basal (□), mid (■) and apical (■) right ventricular free wall site in patients with chronic obstructive pulmonary disease. SR: strain rate. *: $p<0.05$ compared with normal controls; ***: $p<0.001$ compared with normal controls

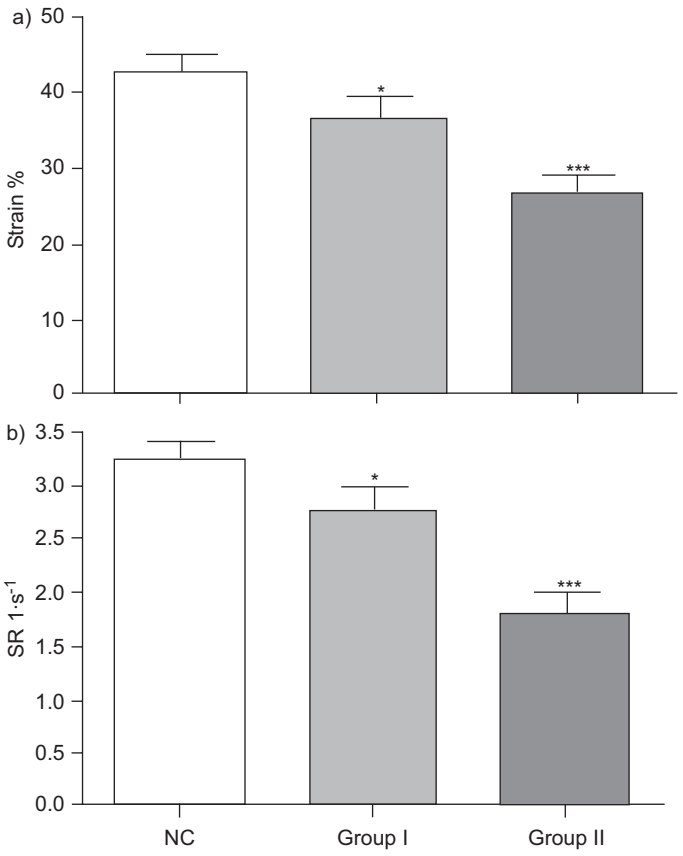

FIGURE 3. Right ventricular peak systolic strain and strain rate (SR) values at basal free wall site in group I (pulmonary artery pressure <35 mmHg) and group II (pulmonary artery pressure >35 mmHg) patients. NC: normal controls. *: $p<0.05$ compared with normal controls; ***: $p<0.001$ compared with normal controls.

factors, such as severity of airflow obstruction, and reflects the interrelationship with deranged pulmonary haemodynamics.

The complexities for estimating RV function are due to several factors. The inaccessibility of the RV behind the sternum often leads to inadequate image quality by conventional imaging modalities and this is particularly pertinent in patients with chronic pulmonary disease who can present with RV dysfunction. Also, the problem of accurately locating the endocardial boundary of the anterior wall of the chamber is compounded by a variable trabeculation pattern, with the apical component having coarser trabeculations compared with the left ventricle. Furthermore, while the left ventricular cavity approximates to an ellipsoid model in healthy subjects, the RV is considerably more complex. The fact that the chamber poorly approximates to any convenient geometric model means that volume calculated with these models only crudely represents true volume [3–5]. Also, myocardial fibre architecture of the left and right ventricles is fundamentally different. Owing to underlying complex RV anatomy, proximal and distal RV portions contract perpendicular to each other: the proximal part (outlet infundibulum) longitudinally and the distal part (inlet chamber or sinus portion) circumferentially. Phylogenetic, embryological and pathological observations support the contention that these areas are distinct components of the heart [12]. Lastly, the shape and performance of the RV depends on extrinsic factors, such as preload, afterload and left ventricular performance.

Right ventricular function by tissue/strain Doppler

An advantage of using TDI to assess RV function is that measurement is independent of geometric assumptions and endocardial border tracing. However, one limitation of TDI is that it does not distinguish between active and passive wall motion, and this has led to the development of the TDI-derived modalities of SRI that measure the rate of regional myocardial deformation. At present, there are only a few animal [32] and clinical [33–35] reports available dealing with RV function, as assessed by strain Doppler echocardiography.

The present study describes the characteristics of ultrasound-based regional deformation indices in patients with COPD and their correlation with pulmonary function tests. In the patients of the current study, reduced regional long-axis shortening was observed in all segments, but function was best preserved in the apical trabecular area of the RVFW and most decreased in the RV basal inlet region. RV long axis function correlated closely with the estimated radionuclide ejection fraction, as well as with the right-sided pressures. This is in accordance with previous reports describing afterload dependence of the

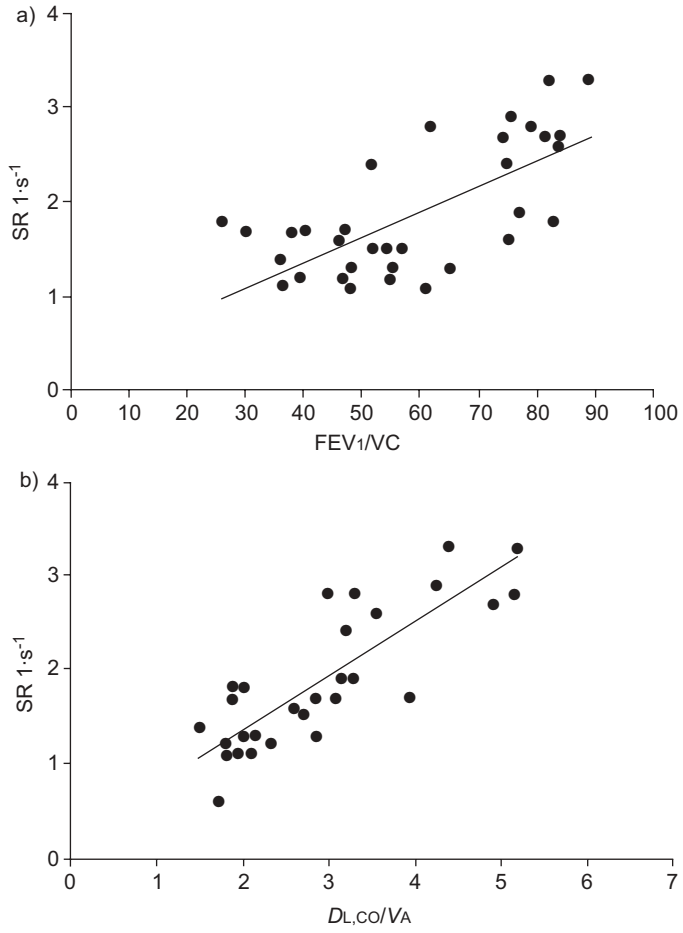

FIGURE 4. Correlation between peak systolic strain rate (SR) at basal free wall site and respiratory function parameters in patients with chronic obstructive pulmonary disease. a) Correlation between SR and forced expiratory volume in one second/vital capacity (FEV_1/VC). b) Correlation between SR and carbon monoxide diffusion lung capacity per unit of alveolar volume ($D_{L,CO}/V_A$).

RV systolic function, mostly represented by ejection fraction [36–38]. Although the myocardial deformation rate and ejection fraction are two different measurements, the current study shows a significant correlation between the peak systolic SR and the RV ejection fraction. In addition, SS and peak systolic SR at basal FW site of 25% and -4 s^{-1} predict a preserved ejection fraction ($\geqslant$0.50) with relatively high sensitivity and specificity. SRI determination had high feasibility in the COPD patients of the current study because it was often measurable in the presence of low-quality 2D RV imaging and also had good reproducibility. Furthermore, in contrast to other ultrasound-based methods of quantifying global RV function, such as the Tei index, SRI potentially allows the quantification of longitudinally systolic and diastolic function for each segment of the right ventricle.

The nonhomogeneity in longitudinal RV function observed in the patients of the current study is presumably a result of the complex anatomy of the RV that is comprised of three morphologically distinct units: a smooth inlet portion, a tubular infundibulum, and a more trabeculated apical portion. As a result of their different muscular arrangements, each could respond differently to both changes in preload and afterload, and fibre stretch as a result of dilatation. When the overall RV function is taken into account, the inlet area of the RV chamber has a greater contribution compared with the trabecular region and the infundibulum. This may explain the nonhomogeneous decrease in systolic deformation that occurs in COPD patients during times of worsening hypoxia, and hence increased afterload stress.

Some overlaps in SRI parameters between patients with and without pulmonary hypertension and controls may have been caused by conduction abnormalities (right bundle branch block on electrocardiography) that occurred in four (18%) patients with pulmonary hypertension, discoordinating wall contraction and complicating the pattern of deformation. Exclusion of such patients could improve the correlation, however, at the cost of marked patient selection.

Limitations

Strain measurements are angle dependent, as are other Doppler modalities, and interpretations of strains should be performed with caution if tissue direction deviates more than 30° from the beam direction. The angle problem is a significant limitation of this technique and repositioning of the transducer can help to avoid the problem.

Strain profiles and curves do not always return to baseline at end diastole. This may be in part due to the mathematical integration algorithm, but may also be caused by the fact that the wall itself does not return to exactly the same state of deformation at the end of the cycle as was the case at the start. This aspect could be related to several factors, including the normal beat-to-beat variation in stroke volume.

Also, current SRI technology is characterised by considerable noise in the SR signal that produces a poorer image quality, especially with higher heart rates, even if averaging the results of three heartbeats [33] can reduce the impact of this limitation. Furthermore, only apical scanning offers comparable information on all segments. This restricts analysis to longitudinal deformation, as well as the effect of loading on SR parameters, which requires further testing.

The correlation of SRI variables and radionuclide data may have been influenced by a limited number of patients undergoing radioisotope studies. However, the assessment of the relationship of SRI parameters to radionuclide results was not a primary aim of the present study and was only included to compare the echocardiographic values with a well validated method for assessing RVEF.

Clinical implications

This study demonstrates the utility of SRI parameters for the evaluation of right ventricular function in chronic obstructive pulmonary disease patients. The new echo technologies show impairment of right ventricular function (with good correlation with radionuclide angiography) that is related to pulmonary hypertension and severity of pulmonary disease, and are more sensitive than conventional echocardiographic parameters. Strain rate imaging indices could provide clinically relevant information on regional changes in right ventricular function

in chronic pulmonary disease and contribute towards an understanding of how the differing structural components of the right ventricle deteriorate after increasing afterload, and how they recover after appropriate therapy.

REFERENCES

1 France AJ, Prescott RJ, Biernacki W, Muir AL, Mac Nee W. Does right ventricular function predict survival in patients with chronic obstructive lung disease? *Thorax* 1988; 43: 621–626.
2 Burgess M, Mogulkoc N, Bright-Thomas R, Bishop P, Egan J, Ray S. Comparison of echocardiographic markers of right ventricular function in determining prognosis in chronic pulmonary disease. *J Am Soc Echocardiogr* 2002; 15: 633–639.
3 Levine RA, Gibson TC, Aretz T, *et al.* Echocardiographic measurement of right ventricular volume. *Circulation* 1984; 69: 497–505.
4 Danchin N, Cornette A, Henriquez A, *et al.* Two-dimensional echocardiographic assessment of the right ventricle in patients with chronic obstructive lung disease. *Chest* 1987; 92: 229–233.
5 Denslow S, Whiles HB. Right ventricular volumes revisited: a simple model and simple formula for echocardiographic determination. *J Am Soc Echocardiogr* 1998; 11: 864–873.
6 Vignon P, Spencer KT, Mor-Avi VV, Weinert L, Lang RM. Evaluation of global and regional right ventricular function using automated border detection techniques. *Echocardiography* 1999; 16: 105–116.
7 Schenk P, Globits S, Koller J, *et al.* Accuracy of echocardiographic right ventricular parameters in patients with different end-stage lung diseases prior to lung transplantation. *J Heart Lung Transplant* 2000; 19: 145–154.
8 Jardin F, Vieilliard-Baron A. Right ventricular function and positive pressure ventilation in clinical practice: from hemodynamic subsets to respirator settings. *Intensive Care Med* 2003; 29: 1426–1434.
9 Nishimura E, Ikeda S. Evaluation of right ventricular function by Doppler echocardiography in patients with chronic respiratory failure. *J Int Med Res* 1999; 27: 65–73.
10 Klein AL, Leung DY, Murray RD, Urban LH, Bailey KR, Tajik AJ. Effects of age and physiologic variables on right ventricular filling dynamics in normal subjects. *Am J Cardiol* 1999; 84: 440–448.
11 Burgess MI, Bright-Thomas RJ, Ray SG. Echocardiographic evaluation of right ventricular function. *Eur J Echocardiography* 2002; 3: 252–262.
12 Geva T, Powell A, Crawford E, Chung T, Colan S. Evaluation of regional differences in right ventricular systolic function by acoustic quantification echocardiography and cine magnetic resonance imaging. *Circulation* 1998; 98: 229–345.
13 Vignon P, Weinert L, Mor-Avi V, Spencer K, Bednarz J, Lang R. Quantitative assessment of regional right ventricular function with color kinesis. *Am J Respir Crit Care Med* 1999; 159: 1949–1956.
14 Florea VG, Florea ND, Sharma R, *et al.* Right ventricular dysfunction in adult severe cystic fibrosis. *Chest* 2000; 118: 1063–1068.
15 Lindqvist P, Henein M, Kazzam E. Right ventricular outflow-tract fractional shortening: an applicable measure of right ventricular systolic function. *Eur J Echocardiography* 2003; 4: 29–35.
16 Meluzin J, Spinarova L, Bakala J, *et al.* Pulsed Doppler tissue imaging of tricuspid annular systolic motion: a new, rapid, and non-invasive method of evaluating right ventricular systolic function. *Eur Heart J* 2001; 22: 340–348.
17 Lindstrom L, Wilkenshoff UM, Larsson H, Wranne B. Echocardiographic assessment of arrhythmogenic right ventricular cardiomyopathy. *Heart* 2001; 86: 31–38.
18 Caso P, Galderisi M, Cicala S, *et al.* Association between myocardial right ventricular relaxation time and pulmonary arterial pressure in chronic obstructive lung disease: analysis by pulsed Doppler tissue imaging. *J Am Soc Echocardiogr* 2001; 14: 970–977.
19 Friedberg MK, Rosenthal DN. New developments in echocardiographic methods to assess right ventricular function in congenital heart disease. *Curr Opin Cardiol* 2005; 20: 84–88.
20 Aoki M, Harada K, Ogawa M, Tanaka T. Quantitative assessment of right ventricular function using Doppler tissue imaging in fetuses with and without heart failure. *J Am Soc Echocardiogr* 2004; 17: 28–35.
21 Alam M, Hedman A, Nordlander R, Samad B. Right ventricular function before and after an uncomplicated coronary artery by-pass graft as assessed by pulsed wave Doppler tissue imaging of the tricuspid annulus. *Am Heart J* 2003; 146: 520–526.
22 Vitarelli A, Conde Y, Cimino E, *et al.* Assessment of right ventricular function by tissue Doppler imaging in patients with chronic obstructive pulmonary disease. *J Cardiac Failure* 2004; 10: Suppl. 4, S32.
23 Kukulski T, Hubbert L, Arnold M, Wranne B, Hatle L, Sutherland G. Normal regional right ventricular function and its change with age: a Doppler myocardial imaging study. *J Am Soc Echocardiogr* 2000; 13: 194–204.
24 Currie PJ, Seward JB, Chan KL. Continuous wave Doppler determination of right ventricular pressure: a simultaneous Doppler catheterisation study in 127 patients. *J Am Coll Cardiol* 1985; 6: 750–756.
25 Bommer W, Weinert L, Neumann A, Neef J, Mason DT, DeMaria A. Determination of right atrial and right ventricular size by two-dimensional echocardiography. *Circulation* 1979; 60: 91–97.
26 Kaul S, Tei C, Hopkins JM, Shah PM. Assessment of right ventricular function using two dimensional echocardiography. *Am Heart J* 1984; 128: 301–307.
27 Nakamura K, Miyahara Y, Ikeda S, Naito T. Assessment of right ventricular diastolic function by pulsed Doppler echocardiography in chronic pulmonary disease and pulmonary thromboembolism. *Respiration* 1995; 62: 237–243.
28 Yeo TC, Dujardin KS, Tei C, Mahoney DW, McGoon MD, Seward JB. Value of a Doppler-derived index combining systolic and diastolic time intervals in predicting outcome in primary pulmonary hypertension. *Am J Cardiol* 1998; 81: 1157–1161.
29 Eidem BW, O'Leary PW, Tei C, Sewaurd JB. Usefulness of the myocardial performance index for assessing right

ventricular function in congenital heart disease. *Am J Cardiol* 2000; 86: 654–658.

30 Vitarelli A, Conde Y, Luzzi MF, *et al.* Transesophageal dobutamine stress echocardiography with tissue Doppler imaging for detection and assessment of coronary artery disease. *J Investig Med* 2001; 49: 534–543.

31 Metz CE. Receiver operating characteristic methodology in radiologic imaging. *Invest Radiol* 1986; 21: 720–733.

32 Jamal F, Bergerot C, Argaud L, Loufouat J, Ovize M. Longitudinal strain quantitates regional right ventricular contractile function. *Am J Physiol Heart Circ Physiol* 2003; 285: H2842–H2847.

33 Weidemann F, Eyskens B, Jamal F, *et al.* Quantification of regional left and right ventricular radial and longitudinal function in healthy children using ultrasound-based strain rate and strain imaging. *J Am Soc Echocardiogr* 2002; 15: 20–28.

34 Dambrauskaite V, Herbots L, Claus P, *et al.* Differential changes in regional right ventricular function before and after a bilateral lung transplantation: an ultrasonic strain and strain rate study. *J Am Soc Echocardiogr* 2003; 16: 432–436.

35 Eysken B, Weidemann F, Kowalski M, *et al.* Regional right and left ventricular function after the Senning operation: an ultrasonic study of strain rate and strain. *Cardiol Young* 2004; 14: 255–264.

36 Nienaber CA, Spielmann RP, Wasmus G, Montz R, Mathey DG, Bleifeld W. Right ventricular ejection fraction from equilibrium Krypton-81m blood pool scans: a noninvasive predictor of pulmonary arterial hypertension. *Eur Heart J* 1987; 8: 297–307.

37 Nagel E, Stuber M, Hess OM. Importance of the right ventricle in valvular heart disease. *Eur Heart J* 1996; 17: 829–836.

38 Lopez-Candales A, Dohi K, Bazar R, Edelman K. Relation of right ventricular free wall mechanical delay to right ventricular dysfunction as determined by tissue Doppler imaging. *Am J Cardiol* 2005; 96: 602–606.